

Rapid Communications

The Rapid Communications section is intended for the accelerated publication of important new results. Since manuscripts submitted to this section are given priority treatment both in the editorial office and in production, authors should explain in their submittal letter why the work justifies this special handling. A Rapid Communication should be no longer than 3½ printed pages and must be accompanied by an abstract. Page proofs are sent to authors, but, because of the accelerated schedule, publication is not delayed for receipt of corrections unless requested by the author or noted by the editor.

Van Hove anomaly in the phonon dispersion of monolayer Ar/Pt(111)

Peter Zeppenfeld, Ulrich Becher, Klaus Kern, Rudolf David, and George Comsa

Institut für Grenzflächenforschung und Vakuumphysik, KFA Jülich,

5170 Jülich, Federal Republic of Germany

(Received 2 January 1990)

Inelastic He scattering has been used to study the surface-phonon dispersion and phonon linewidths of the Ar monolayer physisorbed on Pt(111). As in the previously studied Kr/Pt(111) system a strong vibrational coupling between the adlayer and the Pt substrate is found. In addition, a pronounced enhancement of the linewidth broadening in a narrow region in reciprocal space has been observed, presenting the first experimental evidence of adsorbate coupling to the longitudinal bulk band edge and the longitudinal surface resonance of the Pt substrate due to the Van Hove singularity of the projected phonon density of states.

A few years ago Hall, Mills, and Black¹ explored theoretically the effect of the coupling of the vibrational modes of thin physisorbed films to the phonons of an underlying smooth substrate. They showed that such a vibrational coupling between adlayer and substrate would manifest itself in three distinct features: (a) close to the zone center, where the adlayer mode and the projected bulk bands of the substrate overlap, a damping of the adlayer vibration through an energy transfer into the bulk phonon bands leads to a lifetime shortening and thus a linewidth broadening of the adlayer phonons. (b) A hybridization of the adlayer mode and the substrate Rayleigh wave resulting in an energy splitting at wave vectors Q where the crossover of the two-phonon branches occurs. (c) Likewise a hybridization of the adlayer mode and the longitudinal bulk band edge of the substrate is expected; at this band edge the bulk phonon density of states exhibits a Van Hove singularity of the shape $(\omega - c_l Q)^{-1/2}$.

Two of these theoretical predictions have already been verified experimentally by inelastic He-atom scattering. In the case of Xe adlayers on Ag(111) a linewidth broadening in the first half of the Brillouin zone has been detected by Gibson and Sibener;² they also observed a phonon intensity increase in the crossover region suggestive of a hybridization with the Ag Rayleigh wave. More recently, the hybridization of the adlayer mode and the substrate Rayleigh wave could be resolved experimentally and studied in detail for Kr mono-, bi-, and trilayers on Pt(111).³ Besides this hybridization a linewidth broadening of ~ 0.55 meV for the monolayer and ~ 0.4 meV for the bilayer has been observed in the region where the Kr adlayer mode and the projected Pt bulk bands overlap, demonstrating the strong adsorbate-substrate vibrational

coupling even beyond one monolayer. Meanwhile, the dynamical behavior of other rare-gas adlayers (Xe, Ar) on Pt(111) has been studied experimentally and compared to theory.⁴ Evidence for dynamical adsorbate-substrate coupling has also been obtained recently for Xe monolayers on graphite.⁵ However, so far no experimental evidence for an anomaly due to the hybridization of the adlayer mode and the longitudinal bulk band edge has been reported. Since this hybridization is expected to give "less dramatic anomalous dispersion"¹ it was concluded³ that the effect induced by the coupling to the longitudinal bulk band edge was apparently too small to be resolved within the experimental resolution.

Here we report the first experimental evidence of a Van Hove-type anomaly in the surface phonon dispersion of monolayer Ar on Pt(111). Two distinctive features make the Ar monolayer a likely candidate to reveal this anomaly experimentally: (a) A relatively small linewidth broadening of the Ar phonon in the overlapping region of the projected Pt bulk bands and the adlayer mode and (b) a high enough phonon energy to allow the experimental separation of the intersection of the adlayer mode with the longitudinal bulk band edge from that with the Pt Rayleigh wave.

The experimental data reported below have been obtained with the UHV high-resolution He-scattering apparatus described in detail elsewhere.⁶ The He-beam generator and detector being immobile the total scattering angle is fixed: $\theta_i + \theta_f = 90^\circ$. The angular divergence of the incoming beam and the angle subtended by the detector are both 0.2° . The energy of the incident beam in these experiments was 18.3 meV at an energy spread of 0.25 meV. Time-of-flight (TOF) analysis is performed by

means of pseudorandom chopping with a time resolution of 2.5 μ s, the length of the flight path being 790 mm. Under these conditions the overall energy resolution of the TOF spectrometer is $\Delta E_{\text{instr}} = 0.32$ meV. The overall momentum resolution is about 0.02 \AA^{-1} .

The sample is a high-quality Pt(111) surface with an average terrace width of $\approx 2000 \text{ \AA}$.⁷ The Ar adlayers investigated here were obtained by exposing the Pt surface at 20 K to an Ar pressure of about 5×10^{-8} mbar. When the desired coverage was reached the ambient Ar gas was pumped off and the Ar layer was carefully annealed at 35 K. By a procedure described in Ref. 8 we could show that Ar completely wets the Pt(111) surface and the exposure needed for the completion of successive layers could be determined to within a few percent. The structure of the Ar monolayer has been characterized by He diffraction. On the clean Pt surface Ar condensates into a 2D solid phase with hexagonal symmetry aligned with the Pt(111) substrate (i.e., $\bar{\Gamma}\bar{M}_{\text{Pt}} \equiv \bar{\Gamma}\bar{M}_{\text{Ar}}$). In fact, the submonolayer structure of Ar is rather complicated. For instance, with increasing Ar coverage a phase transition into a high-order commensurate phase is observed at a coverage of about 0.75 of a full monolayer. These results will be discussed in detail in a forthcoming paper.⁹ In the present context it is important to note that the energy-loss measurements have been performed both at full monolayer coverage and in the low-coverage regime. No difference between the results has been detected. Thus, under the present experimental conditions and instrumental resolution a possible influence of the details of the Ar adlayer structure on the dynamical behavior could not be observed.

A typical He-diffraction scan of a full Ar monolayer physisorbed on Pt(111) taken at $T = 20$ K along the $\bar{\Gamma}\bar{M}$ direction is shown in Fig. 1. From the position of the diffraction peaks a lattice constant $a_{\text{Ar}} = 3.70 \pm 0.02 \text{ \AA}$ of the Ar monolayer is deduced. The width of the diffraction peaks⁶ provide an estimate for the average domain width of $\sim 500 \text{ \AA}$.

Figure 2 shows a TOF spectrum of the Ar monolayer taken at an angle of incidence $\theta_i = 40.4^\circ$ along the $\bar{\Gamma}\bar{M}$ azimuth with the TOF-distribution transformed to an

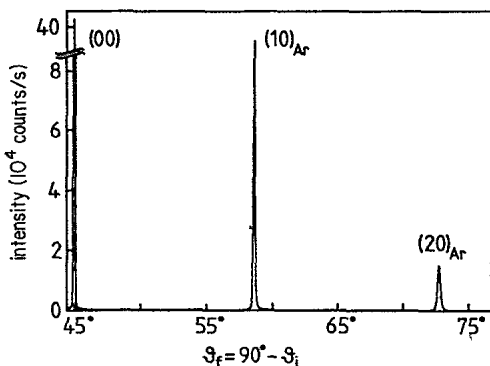


FIG. 1. Polar He-diffraction pattern of an Ar monolayer physisorbed on Pt(111) along the $\bar{\Gamma}\bar{M}$ azimuth. The spectrum was taken with a He-beam energy of 18.3 meV, at a surface temperature $T = 20$ K.

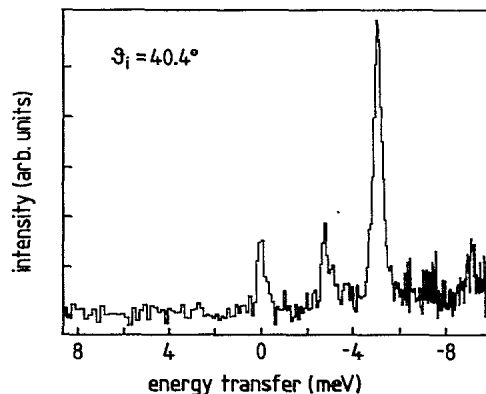


FIG. 2. He TOF spectrum taken at an angle of incidence $\theta_i = 40.4^\circ$ along the $\bar{\Gamma}\bar{M}$ direction at $T = 25$ K. The original time-of-flight distribution has been transformed to an energy-transfer scale. The energy of the primary He beam was 18.3 meV.

energy-transfer scale. The smallness of the elastic contribution (at zero energy transfer) which arises from diffuse scattering from residual surface imperfections and impurities demonstrates the perfectness and cleanliness of the Ar monolayer. The main peak at -5.0 meV results from the creation of an Ar monolayer phonon associated with the vertical Ar-Pt vibration. A second feature is observed at -2.9 meV. The wave vector which is attributed to this phonon loss following the conservation of energy and parallel momentum in the scattering process $Q \approx 0.3 \text{ \AA}^{-1}$ indicates that the phonon is close to the known position of the Pt Rayleigh wave.¹⁰ Note, however, that the Ar monolayer completely covers the Pt surface; therefore, the observation of this phonon originating from the Pt surface Rayleigh wave is already a direct manifestation of the adlayer-substrate coupling.

In Fig. 3, a series of TOF spectra taken at different scattering angles along the $\bar{\Gamma}\bar{M}$ direction are plotted over an energy-loss range from -2 to -6 meV. In these spectra the various features of the dynamical coupling between the adlayer and Pt substrate can be distinguished. As a reference, spectrum (d) taken at $\theta_i = 35^\circ$ corresponds to the creation of an Ar monolayer phonon with wave vector $Q = 0.78 \text{ \AA}^{-1}$, i.e., close to the edge of the 2D Ar Brillouin zone [$Q(\bar{M}) = 0.98 \text{ \AA}^{-1}$]. Since at these large Q values the Pt Rayleigh wave and the Pt bulk phonons have much higher energies than the Ar adlayer mode, no coupling of the Ar phonons to the Pt substrate is expected here. Indeed, the small linewidth $\Delta E = 0.32$ meV of the Ar loss peak at -4.8 meV is determined only by the instrumental resolution ΔE_{instr} of our spectrometer without any measurable additional broadening. Spectrum (a) which is a part of Fig. 2 exhibits two-phonon loss peaks. As already mentioned the feature at -2.9 meV is a signature of the Pt Rayleigh wave dynamically coupled to the Ar adlayer mode. Furthermore, the Ar loss at -5.0 meV is much broader ($\Delta E \approx 0.41$ meV) than in spectrum (d). This difference is due to the fact that the Ar phonon in (a) is created at the center of the Brillouin zone $\bar{\Gamma}(Q = 0.0 \text{ \AA}^{-1})$ where an effective damping of the Ar phonons due to the coupling to the projected bulk pho-

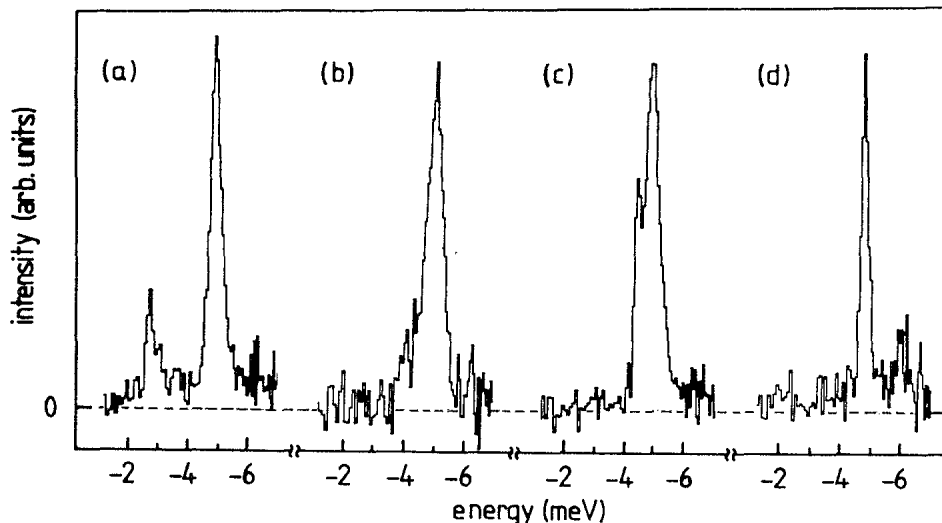


FIG. 3. He TOF spectra taken at different incident angles θ_i along the $\bar{\Gamma}\bar{M}$ direction: (a) 40.4° , (b) 38.5° , (c) 37.7° , (d) 35° ; other experimental parameters as in Fig. 2.

non bands of the Pt substrate occurs. This so called “radiative damping” of the adlayer phonon results in a linewidth broadening $\varepsilon \equiv [(\Delta E)^2 - (\Delta E_{\text{instr}})^2]^{1/2}$ of 0.2–0.3 meV. It is instructive to estimate the corresponding lifetime shortening due to this radiative damping. Using the Heisenberg uncertainty principle $\varepsilon \Delta t = \hbar$ the lifetime becomes $\Delta t \sim 3 \times 10^{-12}$ s. Relating this value to the time scale of the Ar-Pt vibration ($\hbar\omega = 5.0$ meV, i.e., $\nu = 1.2$ THz), a mean phonon lifetime of about three vibrational periods is obtained. Besides the radiative damping also the hybridization of the Ar adlayer mode and the Pt Rayleigh wave is observed experimentally. This is shown in spectrum (c) of Fig. 3. At these scattering conditions ($\theta_i = 37.7^\circ$) corresponding to a wave vector $Q = 0.45 \text{ \AA}^{-1}$ of the Ar phonon the crossing of the adlayer mode and the Pt Rayleigh wave should occur. Instead, due to the hybridization of the two modes this crossing is avoided and a phonon doublet with an energy splitting of ~ 0.8 meV is observed (note also the similar heights of the two peaks).

A compilation of the experimental results obtained from a large number of TOF spectra of the Ar monolayer is shown in Fig. 4. Here the dispersion and the reduced linewidth $\varepsilon = [(\Delta E)^2 - (\Delta E_{\text{instr}})^2]^{1/2}$ of the Ar phonon are plotted against the parallel wave vector Q . From the dispersion curve in Fig. 4(a) the hybridization with the Rayleigh wave (indicated by the solid line) is evident. Also note that the phonon energy at the \bar{M} point is lower by about 0.2 meV as compared to the energy at the zone center $\bar{\Gamma}$. This softening is again a consequence of the dynamical coupling between adlayer and Pt substrate and has also been predicted by theory.⁴

Up to this point we have discussed the results which are analogous to those obtained for Kr monolayers on Pt(111);³ they reflect the same coupling mechanisms as reported earlier. Now we want to focus on an additional feature which is observed in a small range of parallel wave-vector transfer between $Q = 0.25$ and 0.35 \AA^{-1} [see Fig. 4(b)] and which is apparent in spectrum (b) of Fig. 3. Obviously, the half-width of the -5.0 meV Ar loss peak

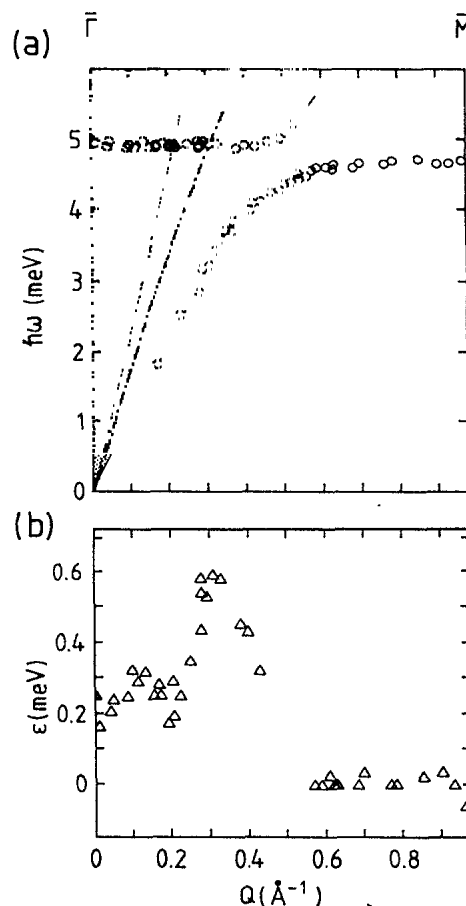


FIG. 4. (a) Experimental dispersion curves from a monolayer Ar on Pt(111) and (b) reduced linewidths of the adlayer phonon as a function of the parallel wave vector Q along the $\bar{\Gamma}\bar{M}$ high-symmetry direction. The shaded area indicates the projected Pt bulk phonon bands. Also indicated are the dispersion of the Pt Rayleigh wave (solid line), the longitudinal Pt bulk band edge (dashed line), and the surface “longitudinal resonance” (dash-dotted line). The Pt phonon dispersion curves were taken from experimental data and theoretical calculations based on these data (Ref. 10).

$\Delta E \approx 0.67$ meV is much larger here than at the zone center [spectrum (a)]. This enhanced peak broadening is not an artifact due to the Pt Rayleigh phonon continuously shifting towards the Ar phonon loss peak with increasing Q . Indeed, the Pt Rayleigh phonon peak in spectrum (b) situated at ~ 4 meV with a height of less than 30% of the Ar loss feature has a negligible influence on the half-width of the Ar peak. Moreover, as can be seen in Fig. 4(b), the peak width of the Ar phonon *decreases* again as the wave vector is raised beyond 0.35 \AA^{-1} , just before the avoided crossing with the Pt Rayleigh wave is observed at $Q \approx 0.45 \text{ \AA}^{-1}$. There is thus another coupling mechanism active at wave vectors ranging from 0.25 to 0.35 \AA^{-1} which gives rise to an extra broadening of about 0.4 meV in addition to the radiative damping of 0.2 – 0.3 meV.

The wave-vector range where this extra linewidth broadening is observed corresponds to the region where the adlayer mode crosses the longitudinal bulk band edge of the Pt substrate.¹⁰ Therefore, we may identify the extra broadening with the anomaly of the phonon dispersion due to the Van Hove singularity of the bulk phonon density of states at the Pt longitudinal bulk band edge. As already mentioned such an anomaly has been predicted by theory,¹ but the results reported here do present the first experimental evidence of this coupling mechanism.

It should be pointed out here that Hall, Mills, and Black do expect a hybridization between the adlayer mode and the longitudinal band edge, similar to the hybridization with the substrate Rayleigh wave, whereas we only observe a linewidth *broadening*. We believe that the energy splitting induced by the hybridization is so small ($\lesssim 0.3$ meV) that the instrumental resolution along with the intrinsic width of the Ar phonon due to the radiative damping does not allow the expected doublet structure to be separated experimentally.

As can be seen from Fig. 4, the wave-vector range from 0.25 to 0.35 \AA^{-1} in which the Van Hove anomaly is observed, appears to be shifted to slightly higher values as would be expected from the crossing of the adlayer mode and the Pt bulk band edge (indicated by the dashed line in

Fig. 4). A possible explanation is given by the fact that on the Pt(111) face a surface resonant mode ("longitudinal resonance")¹⁰ peels off the longitudinal bulk band edge and gives rise to a surface branch lying slightly below the bulk band edge [dash-dotted line in Fig. 4(a)]. It seems very likely that the coupling to the bulk band edge also implies a coupling of the adlayer mode to the longitudinal resonance which crosses the adlayer mode at slightly higher Q values. In conclusion, the coupling of the Ar adlayer mode with the high surface density of states of the longitudinal bulk band edge *and* of the surface longitudinal resonance provides a most plausible explanation of the enhanced linewidth broadening between $Q \approx 0.25$ and 0.35 \AA^{-1} .

Finally, another question should be addressed here: Why is the dispersion anomaly due to the coupling to the longitudinal Pt branches present in the Ar monolayer, whereas in the case of Kr/Pt(111) (Ref. 3) no such effect has been observed? The explanation is probably very simple indeed. While for Kr (and Xe) the effect of the radiative damping on the phonon linewidth is very large [$\epsilon \approx 0.55$ meV for Kr and 0.58 meV for Xe (Ref. 4)] it is rather small in the case of Ar (only about 0.25 meV). Thus, an energy splitting of $\lesssim 0.3$ meV resulting from the hybridization with the longitudinal phonon branches of the Pt substrate leads to an appreciable extra linewidth broadening for Ar but is completely covered by the much larger effect of the radiative damping of the Kr and Xe monolayer phonons. In this sense it is the small radiative damping in the Ar monolayer on Pt(111) which allows the Van Hove dispersion anomaly to be observed experimentally.

In summary, we have shown that the dynamical behavior of the Ar monolayer physisorbed on Pt(111) is significantly affected by the vibrational coupling to the underlying Pt substrate. Besides the "radiative damping" and the hybridization with the Pt Rayleigh wave, a Van Hove-type anomaly due to the coupling to the longitudinal bulk band edge and the longitudinal surface resonance has been observed for the first time.

¹B. Hall, D. L. Mills, and J. E. Black, Phys. Rev. B **32**, 4932 (1985).

²K. D. Gibson and S. J. Sibener, Phys. Rev. Lett. **55**, 1514 (1985); Faraday Discuss. Chem. Soc. **80**, 203 (1985).

³K. Kern, P. Zeppenfeld, R. David, and G. Comsa, Phys. Rev. B **35**, 886 (1987).

⁴B. Hall, D. L. Mills, P. Zeppenfeld, K. Kern, U. Becher, and G. Comsa, Phys. Rev. B **40**, 6326 (1989).

⁵J. P. Toennies and R. Vollmer, Phys. Rev. B **40**, 3495 (1989).

⁶R. David, K. Kern, P. Zeppenfeld, and G. Comsa, Rev. Sci. Instrum. **57**, 2771 (1986).

⁷B. Poelsema, R. L. Palmer, G. Mechttersheimer, and G. Comsa, Surf. Sci. **117**, 60 (1982).

⁸K. Kern, R. David, R. L. Palmer, and G. Comsa, Phys. Rev. Lett. **56**, 2823 (1986).

⁹P. Zeppenfeld, U. Becher, K. Kern, R. David, and G. Comsa, Vacuum (to be published); and (unpublished).

¹⁰K. Kern, R. David, R. L. Palmer, G. Comsa, and T. S. Rahman, Phys. Rev. B **33**, 4334 (1986); V. Bortolani, A. Fanchini, G. Santoro, J. P. Toennies, Ch. Wöll, and G. Zhang, *ibid.* **40**, 3524 (1989).